Energy Proceedings
Vol 36, 2023
ISSN 2004-2965

Research on power generation performance and waste heat utilization of gas-CO_2 combined cycle system

Jingkui Zhang [1, 2], Wen Yan [1], Zhongzhu Qiu[1*], Puyan Zheng[2], Yi Fan[2*], Jiakai Zhang[2*]

1 College of Energy and Mechanical Engineering, Shanghai University of Electric Power, 200090 Shanghai, China

2 Shanghai Non-carbon energy conversion and utilization institute, Shanghai 200240, China
(*Corresponding email: qiuzhongzhu@shiep.edu.cn, yifan0112@shiep.edu.cn)

ABSTRACT

This work proposes a combined cycle, a gas turbine power generation system and a CO_2 cycle power generation system built on the basis of the Ericsson cycle. In this paper, the structure of the combined cycle system is firstly constructed, the temperature-entropy diagram of the gas-CO_2 system is plotted, the simulation model is built on the simulation software platform and its accuracy and validity are verified, and the effects of CO_2 flow rate, pressure ratio, ambient temperature and gas turbine loading rate on the power generation efficiency and primary energy utilization efficiency of the combined system are studied and analyzed. The simulation results have led to the optimal operating conditions of the gas-CO_2 combined cycle, which provides a new technical idea for the future utilization of waste heat energy.

Keywords: gas turbine, CO_2 cycle, combined cycle system, waste heat utilization, electricity production effectiveness

NONMENCLATURE

Abbreviations	
ORC	*Organic Rankine Cycle*
LC	*Low-pressure Compressor*
IC	*Intercooler*
HC	*High-pressure Compressor*
HR	*Reheater*
HH	*High-pressure Heater*
HE	*High-pressure Expander*
LH	*Low-pressure Heater*
LE	*Low-pressure Expander*
HS	*Heat Sink*
LNG	*Natural gas*
GTE	*Gas turbine*
per	*The primary energy recovery*
fer	*The flue gas energy recovery*
Symbols	
Q	*Heat*
W	*Power*
T	*Temperature*
R_g	*Gas constants*
p	*Pressure*
m	*Mass flow rate*
c_p	*Specific heat capacity*
q_m	*Flow rate*
n	*Multivariate index*
φ	*Pressure Ratio*
η	*Efficiency*
ζ	*Heat exchanger efficiency*
H	*High-temperature*
L	*Low- temperature*
net	*Network*
P	*Output power*
C	*Power consumption*
h	*Hot fluid*
c	*Cold fluid*
g	*Flue gas*
in	*Import*
out	*Export*
1,2,3	*Process node*

1. INTRODUCTION

In the future energy system, the construction and operation and maintenance of fossil energy power stations is an indispensable part of power peaking. Compared with coal-fired power generation, gas-fired power generation has the advantages of fast startup, high power density, and high power generation quality, which will play an important role in future energy utilization [1]. So far, researchers have improved the efficiency of gas-fired power plants by hybrid cogeneration, improving the thermal efficiency of gas turbines, and utilizing the low-temperature thermal energy gradient effect [2-5]. In addition, there exists a large amount of waste heat in the gas-fired power generation industry, which can reach temperatures as high as 400-600°C [6], necessitating the development and optimization of various technologies to improve the quality of waste heat energy recovery and utilization. Currently, the mainstream waste heat utilization technologies include Organic Rankine Cycle (ORC), Kalina

This is a paper for the 9th Applied Energy Symposium: Low Carbon Cities and Urban Energy Systems (CUE2023), Sep. 2-7, 2023, Matsue & Tokyo, Japan.

Cycle, Ericsson Cycle, etc. ORC technology is considered as a feasible technological pathway [7], which uses low-boiling-point organic matter as the circulation medium to convert low-grade thermal energy into electrical energy [8]. The Kalina cycle has also played an active role in the field of low-temperature waste heat to power generation, which mainly uses ammonia as the working fluid and is more suitable for hot gas heat sources such as gas turbine exhaust than other heat sources[9]. The Ericsson cycle is rarely mentioned compared to the previous two waste heat to power technologies. It does not have the same history of development as high-power CHP, but because of its high performance at low power levels, it is suitable for several small-scale CHP application sites, such as micro-CHP utilizing solar energy, biomass, etc., or coupling with natural gas combustion systems to form a cogeneration [10-12].

The current mainstream gas-steam combined cycle is a large gas-steam combined cycle power generation system, which is known for its high efficiency, low environmental emissions and many other advantages [13]. However, due to the current gas-steam combined cycle power plant is very large, and for places with small electricity demand, the gas-steam combined cycle power plant is not suitable for the region, so some scholars have proposed a small combined cycle power generation system, small combined cycle power generation system is proposed, not only for the low population density of the region to provide electricity to meet the users of the normal load demand, but also in the high load of electricity can It can also relieve the pressure on the local power grid by shifting peaks and filling in valleys when the power load is high. Small-scale cogeneration has many potential advantages over other large-scale power generation technologies and plays an indispensable role in the industrial, commercial and residential sectors.

The gas-CO_2 combined cycle power generation system mentioned in this paper also consists of a small gas turbine and a CO_2 cycle power generation system, aiming to provide theoretical support for the practical engineering application of small gas waste heat utilization systems.

2. SYSTEM DESCRIPTION

2.1 Ideal thermodynamic model

The ideal Ericsson cycle contains a compressor, expander, and regenerator, with air generally selected as the working medium. Figure 1 describes the system configuration in a closed operating environment, where the cycle working fluid is considered to be air as the ideal gas, and the heat source is mainly high-temperature waste heat from various industries. The cycle covers four main working processes: air is compressed in a compressor. The low-temperature air absorbs heat in a heat exchanger. High-temperature flue gas heat is released into the air. High-temperature and high-pressure air expand in the expander to do work.

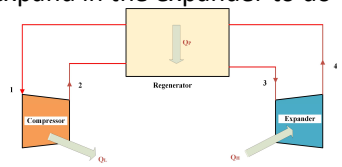

Fig. 1 System composition and working process diagram of Ericsson cycle.

The thermodynamic model of the Ericsson cycle is then introduced. It includes four major processes: two isothermal processes and two isobaric processes. The temperature-entropy drawing of the ideal Ericsson circuit is displayed in Fig. 2 to facilitate the description of this thermodynamic process. Processes 1-2 in Fig. 2 are isothermal compression, where the work mass releases heat to a low-temperature heat source (Q_L). 2-3 are isobaric heating processes, where the work mass absorbs heat in the regenerator (Q_P). 3-4 are isothermal expansion processes, where the work mass absorbs heat from a high-temperature source of heat (Q_H). and 4-1 are isobaric exothermic processes, where the work mass releases heat to the regenerator (Q_P).

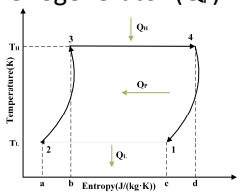

Fig. 2 T-s diagram of Ericsson cycle.

Assuming an ideal regenerator in the circle, the heat released by the heat source during the 4-1 process equals the heat absorbed by the cold source during the 2-3 process. Thus, the area b-3-2-a of the temperature-entropy diagram under the 2-3 path is equal to the area d-4-1-c under the 4-1 path. Commercial regenerators are generally more than 90% efficient, making this assumption reasonable [14]. Subsequently, for the ideal state, the heat transfer relation equation can be formulated as follows:

$$|Q_{41}| = |Q_{23}| \tag{1}$$

Assuming the working mass to be an ideal gas, it can be used the definition of work to derive the energy conservation equation for the input energy during 3-4. Therefore, it can obtain,

$$Q_H = Q_{34} = mR_g T_H \ln \varphi_p \tag{2}$$

where ϕp is the pressure ratio, p_2/p_1.

Likewise, the equation for the transfer of energy from 1-2 to the outside is,

$$Q_L = -Q_{12} = mRT_L \ln \varphi_p \tag{3}$$

For the whole thermal system cycle 1-2-3-4-1, its energy conservation equation is,

$$W_{net} = Q_{net} = Q_H - Q_L \tag{4}$$

Equations (2) and (3) are obtained by substituting them into equation (4),

$$W_{net} = mR \ln \varphi_p (T_H - T_L) \tag{5}$$

2.2 Approximate thermodynamic model

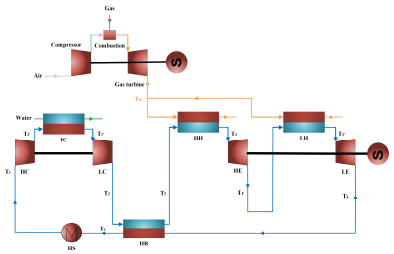

Fig. 3 Schematic Diagram of Gas-CO_2 combined cycle system.

Since the ideal Ericsson cycle is difficult to realize under practical conditions, this paper proposes a gas-CO_2 combined cycle power generation system that approximates the Ericsson cycle, and the schematic diagram of the approximate Ericsson cycle is shown in Fig. 3. In this cycle system, the compression process adopts two-stage compression with intermediate cooling, and the expansion process adopts two-stage expansion with intermediate heating, aiming to replace the isothermal compression and isothermal expansion processes in the ideal Ericsson cycle.

Figure 4 depicts the temperature-entropy diagram of the gas-CO_2 combined circle to provide a clearer understanding of the gas-CO_2 co-generation system. Process 1-2' involves the CO_2 entering the LC, which compresses the CO_2 and increases its temperature to T_2. In process 2'-1', the CO_2 enters the IC, which cools its temperature to $T_{1'}$. The 1'-2' process entails the CO_2 entering the HC, where it is compressed, leading to an increase in temperature to T_2. Next, in processes 2-5, the CO_2 enters the recuperator for heating, causing the temperature to rise to T_5. During processes 5-3, CO_2 and high-temperature flue gas exchange heat in the HH, increasing temperature to T_3. In processes 3-4', high-temperature and high-pressure CO_2 undergo work in the HE, resulting in a decrease in temperature to T_4. Process 4'-3' involves CO_2 and high-temperature flue gas exchanging heat in the LH, increasing temperature to T_3. During process 3'-4, high-temperature and high-pressure CO_2 undergo work in the LE, resulting in a temperature decrease to T_3. process 3'-4 leads to high-temperature and high-pressure CO_2 working in LE, causing a temperature drop to T_4. Process 4-6 involves the heat exchange between the high-temperature outlet CO_2 of LE and HC outlet CO_2 in the HR, reducing the temperature to T_6. Finally, the CO_2 from the heat exchanger is chilled to ambient temperature T_1 by heat transfer with air through the HS and then enters the HC for the next circle.

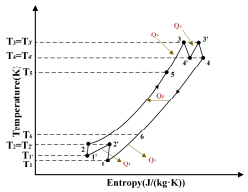

Fig. 4 T-s Diagram of gas-CO_2 combined cycle system.

In the system secondary compression with intermediate cooling work process, according to the definition of work can be two compressor power consumption, the formula is calculated by,

$$W_C = W_{LC} + W_{HC} = \frac{n}{n-1} R_g T_1 \left[1 - \left(\frac{p_2}{p_1} \right)^{\frac{n-1}{n}} \right] + \frac{n}{n-1} R_g T_{1'} \left[1 - \left(\frac{p_3}{p_2} \right)^{\frac{n-1}{n}} \right] \tag{6}$$

where W_{LC} is the power required by LC and W_{HC} is the power required by HC. n is the multivariate index. R_g is the gas constant. T_1 is LC inlet temperature and $T_{1'}$ is HC inlet temperature. p_1 is LC inlet pressure, p_2 is LC outlet pressure and HC inlet pressure, and p_3 is HC outlet pressure.

The external output power of the expansion work process is calculated by,

$$W_P = W_{LE} + W_{HE} = \frac{1}{n-1} R_g T_3 \left[1 - \left(\frac{p_4}{p_3} \right)^{\frac{n-1}{n}} \right] + \frac{1}{n-1} R_g T_{3'} \left[1 - \left(\frac{p_1}{p_4} \right)^{\frac{n-1}{n}} \right] \tag{7}$$

Where W_{LE} is the output work of LE, W_{HE} is the output work of HE. p_3 is the inlet pressure of HE, p_4 is the outlet pressure of HE, and p_1 is the outlet pressure of LE.

In the cooler, the heat absorbed by the process of 2'-1' is calculated by,

$$Q_{IC} = \zeta_{IC} \cdot c_{p,c} \cdot q_{m,c} (T_{2'} - T_{1'}) \tag{8}$$

Where ζ_{IC} is the cooler efficiency. $q_{m,c}$ is the cooling water flow rate. $c_{p,c}$ is the specific heat capacity of water. $T_{2'}$ is the LC outlet temperature and T_1 is the inlet temperature of HC.

The heat input to the system from the waste heat flue gas is calculated by,

$$Q = Q_3 + Q_4 = \zeta_{HH} \cdot c_{p,g} \cdot q_{m,g} (T_{in} - T_{out}) \tag{9}$$

Where ζ_{HH} is the heater efficiency. $c_{p,g}$ is the constant pressure specific heat capacity of the waste heat flue gas. $q_{m,g}$ is the flue gas flow rate. T_{in} is the flue gas inlet temperature and T_{out} is the flue gas outlet temperature.

The heat exchange in the HR is calculated by,

$$Q_r = \zeta_{HR} \cdot c_{p,h} \cdot q_{m,h} (T_4 - T_6) \tag{10}$$

Where $q_{m,h}$ is the hot side CO_2 flow. $c_{p,h}$ hot side CO_2 constant pressure specific heat capacity, It is necessary to determine the flue gas composition to calculate the constant pressure specific heat capacity. T_4 is the hot side inlet temperature, and T_6 is the hot side outlet temperature.

Heat dissipated by the system in the environment can be calculated by,

$$Q_{HS} = c_{p,h} \cdot q_{m,h}(T_6 - T_1) \tag{11}$$

The formula for waste heat flue gas heat is written as,

$$Q_g = c_{p,g} \cdot q_{m,g} \cdot T_{in} \tag{12}$$

The CO_2 circulation efficiency can be calculated by,

$$\eta_{co_2} = \frac{W_P - W_C}{Q} \tag{13}$$

The electricity production effectiveness of a gas-CO_2 cycle system can be calculated by,

$$\eta_{gas-co_2} = \frac{(W_P - W_C) + W_{GTE}}{Q_{LNG}} \tag{14}$$

Where W_{GTE} is the gas turbine generation. Q_{LNG} is the calorific value of natural gas.

The equation for the primary energy utilization of a gas-CO_2 cycle system is，

$$\eta_{\text{per}} = \frac{(W_P - W_C) + W_{GTE}}{Q_{LNG}} \tag{15}$$

The flue gas energy efficiency of the gas-CO_2 cycle is calculated by,

$$\eta_{fer} = \frac{Q_H}{Q_g} \tag{16}$$

2.3 Model verification

A power cycle system from the literature [15] was selected for comparison in this paper to verify the validity of the model. This cycle system is similar to the partial combined cycle system in the CO_2 cycle system used in this paper, but since the working fluid is different, the model is first validated against the literature using air as the working fluid. Using the same parameters as those in the literature (as shown in Table 1), the model simulation results were compared with the calculation results in the literature [15], which are shown in Table 2. It can be seen from Table 2 that the relative error between the simulation results in this paper and the literature values is within ±4%, which indicates that the module used in this paper is reliable, which provides a reliable basis for the joint operation of gas-CO_2 cycle This provides a reliable basis for the joint operation of the gas-CO_2 cycle.

Table 1 Input parameters for the validation model

Parameters	*Value*
air flow	*5.807 kg·s^{-1}*
The inlet temperature of LC	*300 K*
The inlet pressure of LC	*100 kPa*
The inlet temperature of HC	*300 K*
The inlet pressure of HC	*300 kPa*
The outlet temperature of HH	*1400 K*
The outlet temperature of LH	*1400 K*
The inlet pressure of HE	*1000 kPa*
The inlet pressure of LE	*300 kPa*
Compressor efficiency	*0.8*
Expander efficiency	*0.8*

Table 2 Comparison of the simulation results in this paper with those in reference

Parameters	*Literature [15]*	*Results of this article*	*Relative Error*
The power consumption of LC	*806.650*	*803.985*	*0.330%*
The power consumption of HC	*897.240*	*894.664*	*0.287%*
The output power of HE	*1948.829*	*1924.606*	*1.243%*
The output power of LE	*1801.331*	*1779.698*	*1.201%*
The heat exchange HR	*3486.523*	*3371.028*	*3.313%*
The heat exchange HH	*2672.962*	*2641.123*	*1.191%*
The heat exchange LH	*1948.829*	*1927.761*	*1.081%*
Backpressure ratio	*45.435%*	*45.856%*	*0.927%*
Efficiency	*44.274%*	*43.898%*	*0.849%*

3. RESULTS AND CONCLUSION

The design parameters of some of the components of the gas-CO_2 combined cycle power system are shown in Table 3.

Table 3 Parameters of gas-CO_2 co-generation system

Parameters	*Value*
CO_2 *inlet pressure*	*101.3 kPa*
Cooling water temperature	*20 ℃*
Cooling water flow	*10000 kg·h-1*
Compressor efficiency	*0.78*
Expander efficiency	*0.8*
Intercooler efficiency	*0.85*
Heater efficiency	*0.8*
Rated power of gas turbine	*3387kW*

3.1 results

3.1.1 Influence of CO_2 flow rate

First, Figure 5 shows the effect of CO_2 flow rate on power generation in a gas-CO_2 combined cycle system with a CO_2 cycle pressure ratio of 2.0, an ambient temperature of 20°C, and a gas turbine operating at full load. The CO_2 flow rate ranges from 3 kg/s to 17 kg/s. As can be seen in Fig. 5(a), the power generation efficiency of the CO_2 cycle system remains constant between 3 and 7 kg/s as the CO_2 flow rate increases. However, beyond 7 kg/s, the power generation efficiency gradually

decreases. The output power and power consumption of the CO_2 cycle in Fig. 5(b) increase linearly and the maximum net output power of the CO_2 cycle system is 475.905 kW at 15 kg/s. In Fig. 5(c), the power generation rate of the gas turbine remains constant. The power generation efficiency of the gas-CO_2 cycle system initially increases and then decreases. When the CO_2 flow rate reaches 15 kg/s, the maximum value is 31.73%. The maximum percentage of CO_2 cycle power generation to total power generation is 4.24%. Fig. 5(d) shows that for a certain exhaust gas temperature and flow rate, the flue gas outlet temperature of the two heaters decreases and the heat exchange increases as the CO_2 flow rate increases. In addition, it can be seen from Fig. 5(e) that the trend of the primary energy utilization of the system is the same as that of the total power generation rate, and the flue gas utilization of the system increases rapidly with the increase of CO_2 flow rate.

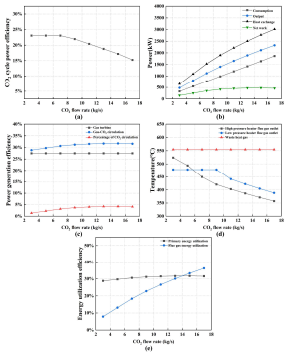

Fig. 5 Variation of thermodynamic parameters at different CO_2 flow rates

3.1.2 Influence of pressure ratio

In this study, the flow rate was set to 15 kg/s, the ambient temperature was 20°C, and the gas turbine was operated at full load. From Fig. 6(a), it can be seen that the power generation efficiency of the CO_2 cycle increases and then decreases with the increase of compression ratio. Fig. 6(b) shows that the power consumption, power output and heat exchange of the CO_2 cycle increase with the gradual increase of the compression ratio. The maximum net output power of the CO_2 cycle is 475.905 kW at a compression ratio of 2.0. The power generation efficiency of the gas-CO_2 cycle from Fig. 6(c) shows an increasing and then decreasing trend. The power generation rate of the gas-CO_2 cycle reaches a maximum value of 31.73% at 2.0, and the contribution of the CO_2 cycle to the total power generation is 4.24%. The primary energy utilization in Fig. 6(e) follows the same trend as the total power generation rate of the system, and the flue gas energy utilization increases with the increase of pressure ratio.

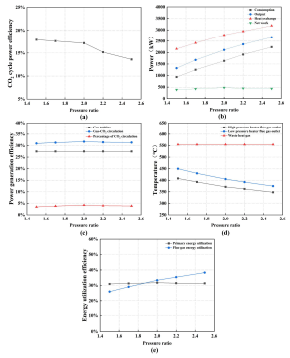

Fig. 6 Variation of thermodynamic parameters at different pressure ratio

3.1.3 Influence of ambient temperature

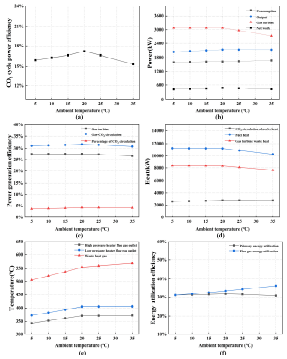

Fig. 7 Variation of thermodynamic parameters at different ambient temperature

In this analysis, the CO_2 flow rate was set at 15 kg/s, the pressure ratio was 2.0, and the gas turbine was operated at full load. From Fig. 7(a), it can be seen that the power generation of the CO_2 cycle increases and then decreases as the ambient temperature increases. Similarly, the power generation rate and total power generation efficiency of the gas turbine show a similar trend as shown in Fig. 7(c). In Fig. 7(b), the output power and net power of the CO_2 cycle show a trend of increasing and then decreasing, with the net output power of the cycle being the largest at 20 °C, and the power generation of the gas turbine decreasing significantly after 20 °C. In Fig. 7(c), the output power and net power of the CO_2 cycle are shown in Fig. 7(d). In Fig. 7(e), the primary energy utilization in Fig. 7(f) follows the same trend as the total power generation efficiency, and the flue gas energy utilization increases with increasing temperature.

3.1.4 Influence of gas turbine load

In the studied gas turbine load, the CO_2 flow rate was set at 15 kg/s, pressure ratio at 2.0 and ambient temperature at 20°C. The gas turbine load was set at rated power of 3387 kW and was operated from 50% of the rated power. From Fig. 8(a), it can be seen that the power generation rate of the CO_2 cycle increases linearly with the increase of the gas turbine load. In Fig. 8(b), the

CO_2 consumption power remains constant and the output power increases linearly. As shown in Fig. 8(d) and Fig. 8(e), the increase in gas turbine load leads to an increase in the temperature of the waste heat flue gas, the gas turbine produces more waste heat, and the heat absorption of the CO_2 cycle increases. In Fig. 8(c), as the gas turbine load increases, the power generation rate of the gas turbine and the gas-CO_2 cycle system increases. In addition, as shown in Fig. 8(f), the primary energy utilization of the gas-CO_2 cycle system increases with the increase of the gas turbine load, while the flue gas energy utilization tends to decrease.

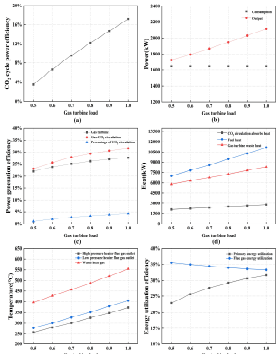

Fig. 8 Variation of thermodynamic parameters at different gas turbine load

3.2 conclusion

In this work, a gas-CO_2 co-generation system based on an approximate Ericsson cycle is proposed to utilize the waste heat from a gas turbine to improve energy efficiency. A thermodynamic evaluation of this combined system yields that the overall power generation efficiency of the system can be improved by appropriately increasing the CO_2 flow rate, choosing the right pressure ratio and the right operating temperature when the gas turbine is at full load, resulting in a higher total power generation rate. Compared with the gas turbine power generation efficiency (27.48%), the gas-CO_2 combined cycle system can achieve a total power generation rate of up to 31.73%. The contribution of the CO_2 cycle system is 4.24%. In the future, power generation, heating and cooling can also be incorporated to fully utilize waste heat resources and further improve energy efficiency.

REFERENCE

[1] Wang G, Bi M, Fan H, Fan Y, Huang C, Shi Y, Liu W, Liu D, Hua H. Key problems of gas‐fired power plants participating in peak load regulation: A review. 2022 IEEE International Conference on Energy Internet (ICEI) 2022; 10:147-152.

[2] Badran O.O. Gas-turbine performance improvements. Applied Energy 1999; 64:263-273.

[3] De Sa A, Al Zubaidy S, 2011. Gas turbine performance at varying ambient temperature. Applied Thermal Engineering 31, 2735-2739.

[4] Liu H, Qin J, Ji Z, Guo F, Dong P. Study on the performance comparison of three configurations of aviation fuel cell gas turbine hybrid power generation system. Journal of Power Sources 2021; 501: 230007.

[5] Kakaras E, Doukelis A, Leithner R, Aronis N. Combined cycle power plant with integrated low-temperature heat (LOTHECO). Applied Thermal Engineering 2004; 24:1677-1686.

[6] Samarasinghe T, Abeykoon C, Turan A. Modelling of heat transfer and fluid flow in the hot section of gas turbines used in power generation: A comprehensive survey. International Journal of Energy Research 2019; 43:1647-1669.

[7] Imran M, Haglind F, Asim M, Zeb Alvi J. Recent research trends in organic Rankine cycle technology: A bibliometric approach. Renewable and Sustainable Energy Reviews 2018; 81:552-562.

[8] Tchanche B.F, Lambrinos G, Frangoudakis A, Papadakis G. Low-grade heat conversion into power using organic Rankine cycles – A review of various applications. Renewable and Sustainable Energy Reviews 2011;15: 3963-3979.

[9] Zhang X, He M, Zhang Y. A review of research on the Kalina cycle. Renewable and Sustainable Energy Reviews 2012; 16:5309-5318.

[10] Creyx M, Delacourt E, Lippert M, Morin C, Desmet B. Modélisation des performances d'un moteur Ericsson à cycle de Joule ouvert. Revista Termotehnica 2014; 1:64-70.

[11] Bădescu V. Optimum operation of a solar converter in combination with a Stirling or Ericsson heat engine. Energy 1992; 17:601-607.

[12] Bonnet S, Alaphilippe M, Stouffs P. Energy, exergy and cost analysis of a micro-cogeneration system based on an Ericsson engine. International Journal of Thermal Sciences 2005; 44:1161-1168.

[13] Shin J.Y, Jeon Y.J, Maeng D.J, Kim J.S, Ro S.T. Analysis of the dynamic characteristics of a combined-cycle power plant. Energy 2002; 27:1085-1098.

[14] Blank D.A, Wu C. Power limit of an endoreversible Ericsson cycle with regeneration. Energy Conversion and Management 1996; 37: 59-66.

[15] Moran M J, Shapiro H N, Boettner D D. Fundamentals of engineering thermodynamics. America: Wiley;2010.